Molybdenum isotope behaviour in groundwaters and terrestrial hydrothermal systems, Iceland

Rebecca A. Neely[1], Sigurdur R. Gislason[1], Magnus Ólafsson[2], Alex J. McCoy-West[3], Christopher R. Pearce[4], Kevin W. Burton[3]

[1]Institute of Earth Science, University of Iceland, IS-101 Reykjavík, Iceland

[2]ÍSOR, Iceland GeoSurvey, Orkugardur, Grensásvegur 9, IS-109, Reykjavík, Iceland

[3]Department of Earth Science, Durham University, Science Labs, Durham, DH1 3LE, UK

[4]National Oceanography Centre Southampton, University of Southampton Waterfront Campus, European Way, Southampton, SO14 3ZH, UK.

Key words groundwater, Hydrothermal, Mo isotopes, ocean mass balance

Abstract

Molybdenum (Mo) isotopes have proved useful in the reconstruction of paleoredox conditions. Their application generally relies upon a simplified model of ocean inputs in which rivers dominate Mo fluxes to the oceans and hydrothermal fluids are considered to be a minor contribution. To date, however, little attention has been paid to the extent of Mo isotope variation of hydrothermal waters, or to the potential effect of direct groundwater discharge to the oceans. Here we present Mo isotope data for two Icelandic groundwater systems (Mývatn and Þeistareykir) that are both influenced by hydrothermal processes. Relative to NIST 3134 = +0.25‰, the cold (<10°C) groundwaters ($\delta^{98/95}Mo_{GROUNDWATER}$ = -0.15‰ to +0.47‰; n = 13) show little, if any, fractionation from the host basalt ($\delta^{98/95}Mo_{BASALT}$ = +0.16‰ to -0.12‰) and are, on average, lighter than both global and Icelandic rivers. In contrast, waters that are hydrothermally influenced (>10°C) possess isotopically heavy $\delta^{98/95}Mo_{HYDROTHERMAL}$ values of +0.25‰ to +2.06‰ (n = 18) with the possibility that the high temperature endmembers are even heavier. Although the mechanisms driving this fractionation remain unresolved, the incongruent dissolution of the host basalt and both the dissolution and precipitation of sulfides are considered. Regardless of the processes driving these variations, the $\delta^{98}Mo$ data presented in this study indicate that groundwater and hydrothermal waters have the potential to modify ocean budget calculations.

1. Introduction

Molybdenum (Mo) is an essential micronutrient and redox sensitive transition metal that provides key information in Earth and environmental studies. Molybdenum stable isotopes have been extensively used as a paleoredox proxy (e.g. Asael et al., 2013; Barling et al., 2001; Barling & Anbar 2004; Archer & Vance 2008; Pearce et al., 2008; Goldberg et al.,

2009; Willie et al., 2008). Despite having generally low concentrations in the continental crust (~1-2 ppm; Taylor and McLennan, 1985), Mo is the most abundant transition metal in the modern oceans (~10 ppb; e.g. Nakagawa et al., 2012, Table 1). This relatively high concentration results from the efficient transport of Mo from the continents to the oceans, due to the solubility of Mo phases under oxidative weathering and the subsequent transport of dissolved Mo prior to its slow removal from the oceans in the presence of dissolved O_2.The resulting residence time of Mo in the oceans of 440 ka (Miller et al., 2011) is more than two orders of magnitude greater than the ocean mixing time, so that the oceans have uniform Mo elemental and isotope compositions (Nakagawa et al., 2012).

Under oxidising conditions Mo is present in solution as the stable molybdate ion, MoO_4^{2-}, (Fig. 2). In this form Mo is slowly removed from the water column through uptake into ferromanganese phases, which preferentially incorporate isotopically light Mo (e.g. Barling et al., 2001; Barling & Andbar 2004; Goldberg et al., 2009; Miller et al., 2011; Wasylenki et al., 2011). As a result of this fractionation the modern oceans are the heaviest Mo reservoir on Earth (Kendall et al., 2016). In contrast, Mo is readily removed from solution in anoxic-sulfidic waters with very little net isotopic fractionation. In the presence of reduced sulfur, Mo forms oxothiomolybdate ions, $MoO_{4-x}S_x^{2-}$, which are highly particle-reactive and thus rapidly removed from solution (e.g. Barling et al., 2001). This behaviour underpins the application of Mo isotopes and abundances as a proxy for past ocean anoxia (e.g. Pearce et al., 2008; Asael et al., 2013).

Early paleoredox studies assumed a comparatively straightforward ocean budget in which Mo input was dominated by the dissolved riverine phase that was assumed to be stable through time and to directly reflect the chemical signature of continental rocks. However, many studies have since demonstrated that the average riverine composition is typically heavier

than the catchment bedrock, both globally (e.g. $\delta^{98}Mo_{GLOBAL\ RIVERS}$ = +0.20‰ to +2.30‰; Archer & Vance 2008) and locally (e.g. $\delta^{98}Mo_{ICELAND\ RIVERS}$ = -0.25‰ to +1.65‰ in a basaltic (<+0.25‰) catchment; Pearce et al., 2010). This enrichment in heavy isotopes in the dissolved phase is attributed to a number of processes including: incongruent dissolution during weathering (e.g. Archer & Vance 2008; Neubert et al., 2011; Voegelin et al., 2012); adsorption of isotopically light Mo to organic phases in soils (e.g. Siebert et al., 2015; King et al., 2016); and, although considered small in terms of mass balance, adsorption of light Mo to riverine particles (e.g. Archer & Vance 2008; Pearce et al., 2010).

In contrast to the dissolved riverine Mo flux, little attention has been paid to the potential contributions of groundwater to Mo in the oceans. Groundwaters may affect seawater chemistry both directly (through submarine groundwater discharge) and indirectly as a significant source of river base flow. Indeed, Pearce et al. (2010) attributed some of the progressive increase in riverine $\delta^{98}Mo$ to the addition of isotopically heavy groundwater. The significance of groundwater contributions to riverine and seawater Mo signatures is poorly constrained due to the paucity of data. To date King et al. (2016) have reported groundwater $\delta^{98}Mo$ data: characterised by isotopically heavy $\delta^{98}Mo$ compositions (+0.25‰ to +0.51‰) relative to the catchment bedrock ($\delta^{98}Mo$ +0.06‰) in Hawaii, attributed to the retention of light isotopes in soils and the preferential leaching of heavy Mo.

In terms of ocean budgets, groundwater contributions to base flow are accounted for in the global riverine discharge. However, the direct contribution of Mo to seawater from submarine groundwater discharge has rarely been taken into account in marine mass balance. Using ^{226}Ra, Moore (1996) demonstrated that submarine groundwater discharge over 350 km of south-eastern coastline of the United States of America contributes up to 40% of the river-water flux. Direct groundwater discharge may therefore contribute a significant proportion of the water flux to the oceans.

At the present day, rivers (potentially including substantial groundwater contributions) are thought to contribute some 90% of oceanic Mo inputs, with the remaining 10% accounted for by chemical exchange in oceanic hydrothermal systems (McManus et al., 2002). For time periods such as the Archean, hydrothermal heat losses were likely much greater than at present (Lowell & Keller 2003). During these time periods the hydrothermal input of Mo may have been more important in the seawater mass balance. Through detailed study of fluid inclusions from identified hydrothermal vents of mid-Archean age in the Barberton formation, South Africa, De Ronde et al. (1997) found that the vent fluids likely had similar chemical signatures to those of modern day vents. Therefore, the study and characterisation of modern hydrothermal systems will enable better constraints to be placed on inputs to the oceans through geologic time.

Data for mid-ocean ridge (MOR) hydrothermal waters are currently limited to a low-temperature (sampling at 25°C, formation fluids ~63°C) flank system on Juan de Fuca. The end-member fluid was estimated to have a composition of δ^{98}Mo +0.8‰ (McManus et al., 2002). However, it is unclear if this signal represents basalt-seawater interaction or if it was inherited from the overlying sediments. Whilst high-temperature hydrothermal systems are not thought to be significant sources of Mo to the oceans (Miller et al., 2011) the only value currently available for a terrestrial hydrothermal system is δ^{98}Mo -3.7‰ (Pearce et al., 2010).

This study presents Mo isotope and elemental data for two groundwater systems, in northeast Iceland, both of which have been influenced by hydrothermal activity along with limited basalt and sulfide samples.

2. Geological Setting and Methods

111 *2.1 Geological Setting*

112 Hydrothermal activity in Iceland is widespread and associated with both active volcanic
113 centres and off-axis fracture systems. The studied groundwater systems (Fig.1) are both
114 meteoric in origin and located in the northern volcanic zone (NVZ), which extends from the
115 centre of Iceland into the North Atlantic Ocean.

116 The first groundwater system is located in the Mývatn area of northeast Iceland (Fig. 1c). It is
117 associated with the volcanic centre of Krafla, an 8 km caldera with a fissure swarm extending
118 50 km to the north and 40 km to the south. The Krafla hydrothermal fields are located within
119 the caldera whilst the Námafjall field lies outside, within the southern fissure swarm
120 (Gudmundsson & Arnórsson 2005). The fluids are dilute (900 ppm to 1500 ppm total
121 dissolved solids; Gudmundsson & Arnórsson 2002, 2005; Kaasalainen & Stefánsson 2012)
122 and are of meteoric origin (based upon δD and $\delta^{18}O$ content; Darling & Ármannsson).
123 Groundwaters in this region have been divided into six distinct groups by Ármannsson et al.
124 (2000) based upon their geographic location, δD, $\delta^{18}O$, and Cl and B concentrations. These
125 classifications are shown in Fig. 1. The most important subset for this study is group V,
126 thought to result from straightforward mixing between cold and geothermal groundwaters
127 (Darling & Ármannsson 1989) they were notably affected by the Krafla fires of 1977 to 1984
128 with their silica content one constituent yet to return to pre-fire values (Ólafsson et al., 2015).
129 In this region there is some debate as to whether the dominant hydrothermal source is from
130 Krafla or Námafjall (e.g. Armannsson et al., 2000; Ólafsson et al., 2015). Most recently
131 Ólafsson et al. (2015) used Cl/B ratios to demonstrate that the, warm, Mývatn groundwaters
132 may be dominated by fluids from the Krafla geothermal system. Due to the utilisation of
133 these fields for geothermal energy each is well characterised, and for this reason they are
134 ideal for investigating Mo behaviour in both cold groundwaters and hydrothermally
135 influenced systems.

136 The second groundwater system, Þeistareykir (Fig. 1b), is located in the westernmost fissure
137 swarm in the NVZ, which is characterised by large normal faults and rift fissures
138 (Sveinbjornsdottir et al., 2013). The high temperature geothermal activity is linked to magma
139 intrusions associated with the most recent volcanic activity ~2500 years ago
140 (Sveinbjornsdottir et al., 2013). Like the Mývatn groundwater system, the fluids are dilute
141 meteoric waters (~750 ppm to 1100 ppm dissolved solids; Óskarsson et al., 2013) from the
142 south of the area (Sveinbjornsdottir et al., 2013).

143 In addition to the water samples, four basalt and three sulfide samples were analysed (Table
144 2). The basalts are from drill core chippings at depth within the Reykjanes hydrothermal
145 system, Iceland (Fig. 1a). Sulfide minerals in Icelandic samples studied here were too finely
146 disseminated to obtain sufficient material for Mo isotope analysis. The samples here are from
147 the main Outokumpu ore, Finland comprising a ∼4 km long, >50 to 350 m wide and ∼10 m
148 thick rectangular-shape sheet of semimassive–massive sulfides. These sulfides are thought to
149 have formed from hydrothermal fluids, perhaps in a mid-ocean ridge setting. Lead isotope
150 data for whole rock and galena samples from the Outokumpu ores define an age of 1943±85
151 Ma, which is indistinguishable from the 1.95–1.96 Ga U–Pb zircon ages for metagabbros and
152 plagiogranites that intrude the ultramafic rocks (Peltonen et al. 2008). Whilst not from the
153 same location as the groundwaters, combined with literature data, these samples allow some
154 insight into the behaviour of Mo isotopes in these common mineral phases

155

156 *2.2 Methods*

157 Groundwater samples (Mývatn: M01 – M20 and Þeistareykir: Þ01 – Þ11) were collected
158 during routine sampling carried out by the Icelandic GeoSurvey (ÍSOR) in conjunction with
159 Landsvirkjun (National Power Company of Iceland) (Kristinsson et al., 2014). Samples for

Mo isotope analysis were filtered (0.2 µm) into 1 L, pre-cleaned, high density polyethylene bottles, acidified and stored in the dark before analysis. Physical properties, sampling conditions, and major- and trace-element concentrations, from Kristinsson et al. (2014), are reproduced in the electronic supplements (Table ES1). All Mo isotope data measured specifically for this study are reported in Table 1.

In situ pH and Eh (redox potential) values, at the measured sampling temperature of the waters, were calculated by PHREEQC version 3.0.6 (Parkhurst & Appelo 2013) using the minteq.v4 database. Redox potential was determined using the measured iron and sulfur speciation and by assuming atmospheric oxygen saturation at the measured water temperature. The results from these approaches were compared and although the absolute values vary depending on the defined redox couple, the relative trends do not. The best approximation of redox shows that oxidised MoO_4^{2-} dominates the groundwaters (Fig. 2), as is known to be the case for most Icelandic waters below 200°C (Arnórsson & Ívarsson 1985).

2.3 Molybdenum isotope chemistry and analysis

Sample preparation and δ^{98}Mo measurements were undertaken in the Department of Earth Sciences at Durham University. Preliminary Mo concentrations were determined by inductively coupled plasma mass spectrometry (ICP-MS). A volume of each sample was then weighed and spiked with a ^{97}Mo-^{100}Mo double-spike to yield a ~1:1 ratio of total spike:natural Mo with 50-100 ng of natural Mo. Basalt samples were powdered in an agate mill before total dissolution of ~50 mg in a concentrated HF:HNO3 mix (1:2). Basalts were spiked before digestion. After complete dissolution the basalts were dried down before re-dissolution in HCl and treated in the same manner as the groundwater samples. Chemical separation of Mo was achieved using a single pass anion exchange procedure detailed in

Pearce et al. (2009), with an additional 12 ml 0.5 M HF matrix elution step to ensure complete removal of Zn before final Mo elution in 3 M HNO_3.

The sulfides: chalcopyrite (0.2 g), pyrrhotite (0.6 g) and pyrite (0.7 g) were dissolved using a combination of HNO_3 and HCl acids before being purified using a double pass through anion exchange columns following the protocol described in Willbold et al. (2017), where dilute ascorbic acid is used during sample loading for optimal Fe removal.

Molybdenum isotope compositions were measured using a multi-collector ICP-MS (Thermo-Finnigan Neptune, Durham University) equipped with an Aridus II desolvating nebuliser. Samples were aspirated at ~35 µl min^{-1} and the maximum sensitivity was ~400 V ppm^{-1}. Measurements were made in low resolution mode using X-cones and static collectors. Analyses consisted of 50 cycles of 4s integrations. Total procedural blanks were <1 ng Mo and data processing was conducted offline using a deconvolution routine (Pearce et al. 2009) based on the Newton-Raphson method.

All Mo isotope compositions are reported in conventional delta notation in parts-per-thousand relative to a reference solution (Eq. 1), with errors given as 2 standard deviations offrom the mean. Given the inconsistent reporting of Mo isotope data in the literature it is important to note that all data, including literature data, are reported relative to SRM NIST 3134 = +0.25‰ (Nägler et al., 2014).

$$\delta^{98/95}Mo = \left[\left(\frac{\frac{^{98}Mo}{^{95}Mo_{SAMPLE}}}{\frac{^{98}Mo}{^{95}Mo_{NIST\ 3134}}}\right) - 1\right] \cdot 1000 + 0.25 \quad (1)$$

Long-term machine reproducibility was determined by measurement of an in-house Romil standard, which gave δ^{98}Mo = +0.30 ± 0.05‰ (2SD, n = 183). The IAPSO seawater standard gave a δ^{98}Mo composition of +2.34 ± 0.08‰ (2SD, n = 43(17) - where n is the number of measurements and in brackets is the number of repeated chemical separations. This is indistinguishable from the mean of published values of +2.33 ± 0.10‰ (given in Goldberg et al., 2013). As this is the first Mo data from Durham University an additional Mo standard (Ou-Mo from the Open University) was run; this gave a mean δ^{98}Mo value of -0.10 ± 0.03‰ (2SD, n = 11), comparable with values obtained from Imperial College London (-0.12 ± 0.04‰) and the Open University (-0.13 ± 0.02‰) (Goldberg et al., 2013). Taken together, these data suggest a long-term external reproducibility (2 s.d.) of ± 0.08‰ or better.

3. Results

Data from this study are presented in Tables 1 and 2. Additional data for the water samples are reproduced in Table ES1 (Kristinsson et al., 2014). Sampling temperatures range from 0°C to 93.2°C and in situ pH is generally alkaline with a mean of 8.4 (Fig. 2) and ranging from 6.9 to 10.0. Aqueous components such as total dissolved solids (TDS), SO_4^{2-}, and SiO_2 increase with temperature with marked increases at temperature over 10°C; therefore, for ease of discussion, samples >10°C are grouped together and considered as hydrothermally influenced groundwaters.

The overall range in Mo concentration in the groundwaters varies from 0.08 ppb to 4.85 ppb (Table 1; Fig. 3). In general, the cold groundwaters (sampling temperature <10°C) contain less Mo than the hydrothermally influenced waters. The Þeistareykir waters (diamonds) have a narrow range of relatively low Mo concentrations (0.08 to 0.22 ppb) whilst the Mývatn waters (circles) range from 0.21 to 4.85 ppb. Curiously, although the group V waters are from

229 the Mývatn groundwater system and are hydrothermally influenced, they have notably lower
230 Mo concentrations (0.21 to 0.37 ppb, Fig. 3) than the other hydrothermal samples.

231 The groundwaters possess a wide range of δ^{98}Mo isotope compositions, from -0.15‰ to
232 +2.06‰ (Table 1, Figs. 4 & 5). The cold Þeistareykir waters are isotopically light, with
233 δ^{98}Mo varying from -0.15‰ to +0.17‰, whilst the more hydrothermally influenced waters
234 are isotopically heavier, up to +0.68‰. Similarly, the cold waters from the Mývatn area range
235 from δ^{98}Mo +0.18‰ to +0.47‰ whilst the hydrothermally influenced waters are heavier:
236 between +0.47 and +2.06‰. The exception to this is sample M03 (LUD-4), a cold water well
237 with a high Mo concentration (1.52 ppb), heavy Mo isotope composition of +1.12‰ (Table
238 1, Fig. 4), and distinctive chemistry including, for example, elevated TDS, SO_4^{2-}, and Al
239 (Table ES1).

240 The basalts contain between 0.14 ppm and 1.01 ppm Mo, with the hyaloclastite having the
241 highest concentration of 4.67 ppm Mo (Table 2). In comparison, the chalcopyrite contains an
242 order of magnitude more Mo, some 38 ppm, whilst the pyrite and pyrrhotite contain
243 0.074 ppm and 0.048 ppm, respectively. The basalts are isotopically light, ranging from
244 +0.16‰ to –0.12‰, whereas the sulfides are all isotopically heavy; the chalcopyrites are
245 +1.16‰ and the pyrite and pyrrhotite +1.80‰ and +1.46‰, respectively.

246

247 **4. Discussion**

248 *4.1. Cold groundwaters*

249 Generally, in the cold Icelandic groundwaters investigated here, as the Mo concentrations
250 increase the isotopic composition becomes increasingly heavy (Fig. 4). However, with the
251 exception of sample M03, the cold groundwaters show only a small degree of fractionation

252 away from the average composition of Icelandic basalts (Fig. 4). Icelandic basalts,
253 specifically, are isotopically light and in this study they have compositions that range from
254 $\delta^{98}Mo_{BASALT}$ +0.16‰ to -0.12‰, comparable with published data for Icelandic lavas of
255 +0.1‰ (Yang et al., 2015). The cold Þeistareykir samples are also isotopically light (-0.15‰
256 to +0.17‰), similar to the down-well Icelandic basalts measured in this study (Fig. 4).

257 The mean δ^{98}Mo value of the cold groundwaters at Þeistareykir is -0.01‰ and at Mývatn,
258 +0.35‰. These values are comparable to the basalt-hosted Hawaiian groundwaters measured
259 by King et al. (2016), which have a mean Mo isotope composition of +0.39‰ (range:
260 +0.25‰ to +0.51‰) (Fig. 4). Whilst the waters are isotopically similar, the Mo
261 concentrations in the Icelandic groundwaters are almost an order of magnitude lower than
262 those in Hawaii. The Hawaiian groundwater Mo concentrations range from 1.83 ppb to 4.86
263 (mean: 3.0 ppb) whilst the maximum Mo in the cold Icelandic waters is 1.52 ppb with a mean
264 of 0.5 ppb (slightly higher than the 0.2 ppb mean of 150 cold groundwaters from an earlier
265 study in north Iceland; Árnórsson & Óskarsson 2007).

266 The Icelandic groundwaters are within the range of Mo isotope values measured in rivers
267 both locally, in Iceland (δ^{98}Mo from -0.25‰ to +1.65‰ (Pearce et al., 2010), and globally
268 (-0.10‰ to +2.30‰; summarised in Kendall et al. (2016)). However, on average they are
269 lighter than the global riverine mean of δ^{98}Mo +0.7‰ (Archer & Vance 2008) (Figs. 4 & 8)
270 and the Iceland riverine mean of +0.6‰ (Pearce et al., 2010). If the proportion of direct
271 groundwater discharge is anywhere close to the 40% of river discharge, as suggested by
272 Moore (1996), and the global groundwater mean is isotopically lighter than that of the global
273 river discharge, as indicated by these data and that of King et al. (2016), then the overall input
274 to the oceans may need to be revaluated (see section 4.4). We recognise, however, that
275 current groundwater δ^{98}Mo data remain limited both in terms of their geological setting and
276 their host lithologies.

4.2. Groundwater Mixing

As with all groundwaters, the chemistry of the Þeistareykir and Mývatn waters is determined by the composition of the source, precipitation, degree of water-rock interaction, mixing with other waters, and the introduction of volcanic gasses (Ármannsson et al., 2000). In the case of these two systems, the influence of hydrothermal waters is significant with mixing and, to a lesser extent, steam-heating known to be important controls on chemistry (Darling & Ármannsson 1989; Ólafsson et al., 2015).

For the Mývatn waters, the cold groundwater endmember is represented by M07, Garðslind (Fig. 5; Table 1). It is one of the largest cold-water springs in the region and represents the non-hydrothermally influenced endmember (Ólafsson et al., 2015). It is not possible to account for all of the Mývatn groundwater data with one binary mixing model (Fig. 5), suggesting that either there are two distinct hydrothermal endmembers, or else that the chemistry of these waters is not controlled by mixing alone. The most recent work on the origin of these groundwaters (Ólafsson et al., 2015) concluded that the warm waters may be related to the Krafla hydrothermal fluids as opposed to Námafjall. Sample M17 is therefore taken to represent a geothermal endmember; it is isotopically heavy, has a relatively high Mo concentration (1.4 ppb), and negligible Mg, as is characteristic of hydrothermal waters.

Mixing between these two endmembers can account for the majority of the Mývatn groundwaters (solid line; Fig. 5). However, the group V waters do not fit this trend (dashed line; Fig. 5); instead they require an isotopically heavy but low Mo concentration endmember. The low Mo concentration is somewhat surprising as these waters are thought to result from straightforward mixing between cold and geothermal groundwaters (Darling & Ármannsson 1989) and Mo is known to be enriched in geothermal waters compared with cold groundwaters and surface waters (Arnórsson & Ívarsson., 1985). Therefore, there may have

been loss of light Mo to account for the low Mo concentrations seen in these three group V waters.

Ólafsson et al. (2015) argued that these warm waters are, in part, formed as a consequence of steam-heating. Although the behaviour of Mo in the steam (vapour) phase remains poorly understood and data on the isotope composition are limited, it has been suggested that lighter Mo isotopes accumulate in the vapour whilst heavier isotopes remain in the brine (Kendall et al., 2016). This is consistent with preliminary measurements of the vapour phase in geothermal systems from Iceland. All show preferential partitioning of light Mo into the vapour but the Mo concentrations in the vapour phase are relatively low, from 0.30 to 3.27 ppb (Neely et al., 2015).

As Mo can fractionate isotopically on partitioning into a vapour phase, it is possible that this process has influenced the composition of the hydrothermally affected waters. Steam-heating would add isotopically light Mo which cannot explain the isotopically heavy hydrothermal waters. But the loss of steam could leave a residually heavy fluid phase (although this would not explain the high Mo concentrations). Combined with the indication of relatively low Mo concentrations in the vapour (Neely et al., 2015) this suggests that steam-heating alone is not a dominant control on the Mo composition of these waters, in agreement with the conclusions of Ólafsson et al., 2015.

4.3. Controls on hydrothermal endmember Mo composition

Few minerals contain Mo as a major constituent. Of these sulfides such as molybdenite (MoS_2) and pyrite (FeS_2) dominate, with molybdenite containing approximately 60% Mo by weight and often dominating the mass balance in mineralising systems (Kendall et al., 2016). The association of Mo and S in sulfides and the high solubility of their oxidised species (MoO_4^{2-} and SO_4^{2-}) indicates that they can be effectively mobilised during oxidative

weathering. Indeed, based on a similar positive correlation to that shown in Fig. 3, Miller et al. (2011) concluded that pyrite weathering is the dominant source of Mo to modern day rivers. The observed agreement between the groundwater data presented in this study and global river data (Fig. 3) may therefore indicate that groundwater Mo in Iceland is similarly controlled by pyrite and sulfide dissolution.

However, the concentration of Mo in mid-ocean ridge basalt (MORB) sulfides appears to be much lower than continental sulphides (~0.15 ppm; Patten et al., 2013). This suggests that igneous sulfides may not be a significant source of Mo in this setting, consistent with the low Mo concentrations reported in this study for hydrothermal pyrite and pyrrhotite (see Table 2). In contrast, chalcopyrite may be a significant Mo host, containing 38 ppm Mo (Table 2). Molybdenum is also preferentially incorporated into minerals containing Ti^{4+} and Fe^{3+}, so that in basaltic and silicic igneous rocks Mo is often concentrated in ilmenite, titano-magnetite (~10 ppm), and sphene. Relatively high Mo concentrations are also found in olivine (~10 ppm), but are lower in pyroxenes (~0.4 ppm) and plagioclase (~0.2 ppm) (see Arnórsson & Óskarsson, 2007). Arnórsson & Óskarsson (2007) found groundwaters to be more concentrated in Mo than comparable surface waters and, in general agreement with this study, that Mo concentration tends to increase with increasing temperature. They concluded that the main source of Mo to Icelandic groundwaters is the incongruent dissolution of basalt, dominated by plagioclase and to a lesser extent pyroxene and basaltic glass due to Mo retention in titano-magnetite and olivine.

As the main source of Mo is likely to be from the dissolution of the isotopically light host basalts, some process is needed to explain the heavy hydrothermal endmember compositions (Fig. 5). There are several processes that could potentially drive the observed fractionation of Mo isotopes in the warm geothermal waters: (1) pedogenesis; (2) changes in redox state; (3) dissolution of primary minerals; (4) the formation of secondary minerals; and (5) the

dissolution or precipitation of sulfides. To explain the dominant mixing trend in the Mývatn waters (solid line; Fig. 5) the geothermal end member requires an additional source of isotopically heavy Mo whilst the minor, group V endmember mixing (dashed line; Fig. 5) may require loss of isotopically light Mo.

Soils: The retention of light Mo isotopes in soils has been recognised as an important process in driving the preferential enrichment of heavy Mo isotopes in the dissolved phases of pore water, rivers and groundwaters (e.g. Pearce et al., 2010; Siebert et al., 2015; King et al., 2016). Siebert et al. (2015) and King et al. (2016) used selective extraction techniques to show that soil-bound Mo is associated with organic matter and a silicate and/or Ti-oxide residue, as opposed to Mn-Fe oxyhydroxides. However, soils in the NVZ of Iceland are generally thin and sandy with much of the groundwater catchment described as a sand desert, from Vatnajökull glacier in the south to the Atlantic Ocean in the north (see Fig. 5 in Arnalds et al., 2001). Furthermore, as shown in Fig. 6, the *in situ* partial pressures of CO_2 in the cold groundwaters (from 10^{-6} to $10^{-3.6}$ bars) are less than that of atmospheric pCO_2 ($10^{-3.4}$ bars). This suggests that the dissolution and precipitation reactions in these waters take place in isolation from the atmosphere and with little CO_2 contribution from soils (see Fig. 4 in Gislason & Eugster 1987). Consequently it is unlikely that soils exert a significant control on groundwater composition in this region due to their lack of development and coverage.

Redox State: The Eh is relatively difficult to constrain due to the challenges involved in preserving speciation for later laboratory analysis (as demonstrated for Fe speciation in thermal waters; Kaasalainen et al., 2016). For this reason, redox potential was calculated using several approaches and redox pairs. While absolute values of Eh differ between these approaches the speciation in all of the groundwaters is dominated by molybdate, MoO_4^{2-} (Fig. 2). A couple of the samples approach thiomolybdate speciation ($MoO_{4-x}S_x^{2-}$) and removal of thi isotopically light (e.g. Tossell 2005) species could leave the residual fluids isotopically

heavy. However, despite spanning a wide range of Eh values, the redox conditions do not appear to directly account for the isotope composition of dissolved Mo with no trend seen between redox potential and the Mo composition of the groundwaters (Table 1).

Primary minerals: Redox potential can affect the stability and saturation state of mineral phases and dissolution of basalt is thought to be incongruent with respect to Mo (e.g. Arnórsson & Óskarsson 2007; Voegelin et al., 2012). Data on the Mo isotope composition for individual minerals remains limited, but there may be significant isotope variation between phases. Initial data from Voegelin et al. (2014) indicate that hornblende and biotite are up to 0.6‰ lighter than bulk-rock. Maintenance of mass balance therefore requires other phases to be isotopically heavier, and enhanced dissolution of these phases could be responsible for the heavier Mo isotope composition and increasing Mo concentration of the main geothermal endmember (M17). Indeed, Voegelin et al. (2012) found, in both field (stream catchment) and basalt leach experiments, that the preferential weathering of mineral phases, such as magmatic sulfides, resulted in the enrichment of isotopically heavy Mo in the aqueous phase relative to the basaltic bedrock.

An assessment of the saturation state of primary basalt minerals in the groundwaters was made using the PHREEQC database (Parkhurst & Appelo, 2013). Plagioclase, hydrated basaltic glass, and olivine tend to be undersaturated - suggesting the potential to dissolve - whilst pyroxene and magnetite remain oversaturated – suggesting that these minerals are stable and unlikely to dissolve (Fig. 7, Table ES2). As temperature increases, the tendency for forsterite dissolution becomes dominant over plagioclase, coinciding with increasingly heavy Mo isotope signatures. If olivine retains heavier Mo than plagioclase then incongruent dissolution of these phases may control the Mo isotope signatures of these waters. However, additional Mo isotope data on mineral separates are required to assess this hypothesis and it

399 seems unlikely that any individual phase could be isotopically heavy enough and in sufficient
400 abundance to generate 2‰ variations without other processes playing a role.

401 *Secondary minerals*: The formation of secondary phases provides a potential mechanism to
402 remove light Mo from solution (as may account for the group V waters). The formation of
403 secondary phases has been used to explain some of the Mo isotope variation in rivers, with
404 adsorption of light Mo onto Mn-Fe oxyhydroxides driving the waters to heavier values (e.g.
405 Archer & Vance, 2008; Miller et al., 2011). In this study, the most common Mn phases are
406 significantly undersaturated in the groundwaters (Table ES2), whilst Fe phases only tend to
407 be oversaturated in the cold groundwaters. From the calculated saturation indices, there is no
408 indication that the formation of these secondary phases in the group V waters is any more
409 likely than in the other hydrothermal waters (Table ES2). With the hydrothermally influenced
410 waters undersaturated for both Fe- and Mn- oxyhydroxides, their formation is considered to
411 exert little influence on Mo isotopes in these groundwaters.

412 *Sulfides*: Calculating the saturation state of sulfide minerals in the cold groundwaters is
413 difficult due to the absence of measureable reduced S in the system (Table 1; ES1). However,
414 the oxidising nature of these fluids (Fig. 2) would suggest that they are undersaturated with
415 respect to sulfide minerals. It is known that the mixing of hydrothermal waters with cold
416 waters leads to molybdenite undersaturation and therefore favours dissolution of Mo sulfides
417 (Arnórsson & Ívarsson 1985). Consequently, the main mixing trend in Fig. 5 could, in part,
418 be explained by the dissolution of sulfide phases, increasing the Mo concentration in these
419 waters. Molybdenites show a large isotopic variation, ranging from $\delta^{98}Mo_{MOLYBDENITE}$ -1.4‰
420 to +2.6‰ (Breillat et al., 2016) and the hydrothermally sourced chalcopyrite, pyrite, and
421 pyrrhotite measured in this study are all isotopically heavy ($\delta^{98}Mo$ = +1.15 to +1.8‰; Table
422 2, Fig. 8). The dissolution of sulfide phases could be a source of heavy Mo to the
423 hydrothermal endmembers. However, saturation state calculations systematically show that

424 the hydrothermally influenced waters are oversaturated for sulfide minerals (Table ES2),
425 indicating that they are stable and that dissolution is unlikely. Therefore, sulfides are unlikely
426 to be controlling the composition of the main hydrothermal endmember (M17).

427 Alternatively, it is possible that the precipitation of sulfides from reducing, sulfide-bearing
428 waters may instead remove Mo from solution as indicated by the minor group V mixing trend
429 (Fig. 5). When redox is defined using sulfur speciation and trace levels of H_2S are assumed to
430 be present in the hydrothermally influenced waters (at levels of 0.01 ppm to 0.01 ppb) then
431 the hydrothermal samples tend towards sulfide (molybdenite, pyrite, and chalcopyrite)
432 saturation (Table ES2). Whilst molybdenite has not been found in active geothermal systems
433 in Iceland, it is known to occur in some New Zealand geothermal systems and has been
434 identified in hydrothermally altered Tertiary basalt formations at Reydarártindur in southeast
435 Iceland (Árnorsson & Ívarsson 1985). Although the sulfides measured in this study are all
436 isotopically heavy and the compiled molybdenite data show a range from -1.4‰ to +2.6‰
437 (Breillat et al., 2016), Tossell (2005) calculated that aqueous Mo-sulfide complexes are some
438 2‰ lighter than oxidised complexes. Greber et al. (2014) also suggested that light Mo is
439 preferentially incorporated in molybdenite during crystallization leaving behind a residually
440 heavier hydrothermal fluid. If isotopically light, sulfide formation could generate the M14
441 endmember and the group V waters, but cannot be responsible for the main groundwater
442 trend.

443 In the absence of isotope data for sulfides local to the study sites, it is not clear what role, if
444 any, sulfide plays in controlling the Mo chemistry of the waters. Sulfides span a large isotope
445 range and are only sometimes significant hosts of Mo. Although sulfide dissolution and
446 precipitation are potentially contributing factors to the Mo chemistry of these waters, due to
447 the saturation state calculations it is considered more likely that sulfides are stable or forming
448 in these waters, thereby unlikely to be contributing Mo to solution.

449 The mechanisms controlling the compositions of these waters appear to be complex. There
450 are potentially two distinct hydrothermal endmembers as shown on the mixing diagrams (Fig.
451 5): both are isotopically heavy but one possesses high Mo concentrations and the other low
452 concentrations. We suggest that an important control on Mo in the groundwaters is the
453 incongruent dissolution of basalt. The hydrothermal waters are increasingly influenced by the
454 dissolution of olivine over plagioclase, with correspondingly heavier Mo isotope
455 compositions as temperature increases. However, it is unlikely that primary mineral
456 dissolution alone could control the composition of the hydrothermal endmember as it would
457 require extraordinary fractionation between these minerals at high temperatures when
458 forming the basalts. The group V waters are likely to be more strongly influenced by Mo
459 removal mechanisms involving the precipitation of isotopically light phases, such as
460 molybdenite or other sulfide minerals.

461 *4.4. Ocean mass balance*

462 Although the mechanisms responsible for the observed Mo isotope composition in
463 groundwater remain complex, the new data allow a more detailed assessment of the Mo
464 budget of the oceans. Typically, the source of Mo to the ocean is considered to be dominated
465 by rivers, with a minor (~10%) hydrothermal component contributing the remaining flux
466 (McManus et al., 2002), and the sinks of Mo comprise euxininc, suboxic, and oxic
467 sedimentary deposition (e.g. Kendall et al., 2016). There are currently two approaches to
468 evaluating the Mo input composition: (1) the assumption that over long time scales the
469 riverine flux will represent the average crustal value (e.g. Asael et al., 2013); and (2) the
470 direct measurement of the riverine compositions (e.g. Archer & Vance 2008). These two
471 approaches result in slightly different estimates of the Mo isotope input to the oceans. The
472 continental crust has a bulk composition of between δ^{98}Mo +0.35‰ and +0.6‰ and a
473 maximum of +0.4‰ for the upper continental crust alone (Willbold et al., 2017). The riverine

474 average has a higher δ^{98}Mo value of +0.7‰ (Archer & Vance 2008) and when combined in
475 mass balance with a poorly constrained hydrothermal input of δ^{98}Mo +0.8‰ (McManus et
476 al., 2002) results in a Mo input of ca. +0.7‰ (Eq. 2).

477

478 $$\delta^{98}Mo_{input} = f_{river} \times \delta^{98}Mo_{river} + f_{hydrothermal} \times \delta^{98}Mo_{hydrothermal} \quad (2)$$

479

480 If, as the data from these Icelandic cold groundwaters suggest (see section 4.1), the
481 concentration of Mo in groundwaters is similar to that of rivers, and groundwater discharge is
482 the equivalent of 40% of the riverine water flux as suggested by Moore (1996), then
483 groundwaters may account for nearly 30% of the total Mo flux to the oceans (e.g. Rivers:
484 65%; Groundwater: 27%; Hydrothermal: 8%). The available Mo isotope data for
485 groundwaters indicate that they are isotopically lighter (δ^{98}Mo +0.2‰ for the data in this
486 study and King et al. (2016)) than river compositions, thus necessitating a re-evaluation of the
487 Mo ocean input (Eq. 3).

488

489 $$\delta^{98}Mo_{input} = f_{river} \times \delta^{98}Mo_{river} + f_{hydrothermal} \times \delta^{98}Mo_{hydrothermal} + f_{groundwater} \times \delta^{98}Mo_{groundwater} \quad (3)$$

490

491 The result is a Mo input to the oceans of δ^{98}Mo +0.55‰ which, if correct, brings this
492 combined Mo input closer to that of the estimate based upon crustal values. Furthermore, the
493 data from King et al. (2016) indicate that groundwaters can contain around four times more
494 Mo than the riverine average, in which case their contribution ($f_{groundwater}$) would increase,
495 potentially even becoming the dominant source**,** and the total Mo input would be lighter still,

more closely matching that of the crustal values. However, while groundwater data remain limited both in terms of potential flux to the oceans and the isotope composition it is not possible to accurately constrain these values.

Despite high temperature hydrothermal systems generally not being considered a significant source of Mo to the oceans these terrestrial hydrothermal systems maintain relatively high Mo concentrations (up to 4.8 ppb). Without exception, in this study there is preferential enrichment of heavy δ^{98}Mo in the hydrothermal fluid, with minimum δ^{98}Mo in endmember fluids of more than +2‰. If this is indicative of the processes contributing to the evolution of MOR hydrothermal fluids then the hydrothermal portion of the Mo input to the oceans may be heavier than previously estimated. Within the modern ocean budget hydrothermal contributions of Mo are minor; increasing the hydrothermal Mo isotope composition to an extreme of δ^{98}Mo +2.0‰ only increases the combined input ($\delta^{98}Mo_{input}$) by some 0.1‰. However, during early periods of Earth's history, when hydrothermal fluids may have comprised a greater proportion of total inputs to the ocean, the accurate characterisation of these fluids is of greater importance for the interpretation of ocean chemistry. With only one other direct study of hydrothermal fluids, the significance of these systems and reactions at both low and high temperatures remains, at best, uncertain (cf. McManus et al., 2002).

5. Conclusions

We present a comprehensive study of the Mo isotopic composition of waters from two hydrothermally influenced groundwater systems in northeast Iceland with variations in δ^{98}Mo from -0.15‰ to +2.06‰. Although data are currently limited to the basaltic terrains of Hawaii and Iceland, this study represents an important increase in the available data for both cold and hydrothermally influenced groundwaters, with the main findings being:

1) Cold groundwaters in Iceland are isotopically light, ranging from δ^{98}Mo -0.15‰ to +0.47‰ (mean: $\delta^{98}Mo_{GROUNDWATER}$ +0.18‰), and are comparable with the Mo composition of groundwaters from Hawaii (mean δ^{98}Mo +0.39‰) reported in King et al. (2016). On average the groundwaters are isotopically lighter than rivers and have Mo isotope signatures that are similar to their basaltic host-rocks ($\delta^{98}Mo_{BASALT}$ -0.12‰ to +0.16‰).

2) The majority of hydrothermally influenced groundwaters in this study have higher dissolved Mo concentrations (up to 4.81 ppb) and heavier Mo isotope compositions than the regional cold groundwaters ($\delta^{98}Mo_{HYDROTHERMAL}$ +0.25‰ to +2.06‰). Mixing between the cold groundwaters and hydrothermal endmembers (+2.06‰ and +1.08‰) is the main control on the Mo composition of the groundwater samples. The incongruent dissolution of basalt and dissolution and precipitation of sulfide minerals are both processes capable of controlling hydrothermal endmember Mo compositions.

3) With the inclusion of a direct groundwater contribution to the Mo flux to the oceans the combined groundwater and river input is re-evaluated to δ^{98}Mo +0.55‰, in closer agreement with estimates based upon the crustal composition alone. However, whilst groundwater data remain limited these estimates should be considered with caution.

References

1. ARNALDS, O., GISLADOTTIR, F. O. & SIGURJONSSON, H. 2001. Sandy deserts of Iceland: an overview. Journal of Arid Environments, 47, 359-371.
2. ARCHER, C. & VANCE, D. 2008. The isotopic signature of the global riverine molybdenum flux and anoxia in the ancient oceans. Nature Geoscience, 1, 597-600.
3. ÁRMANNSSON, H., KRISTMANNSDÓTTR, H. & ÓLAFSSON, M. 2000. Geothermal influence of groundwater in the Lake Mývatn area, North Iceland. In *Proceedings of World Geothermal Congress 2000 (pp. 515-20).*
4. ARNÓRSSON, S. & ÍVARSSON, G. 1985. Molybdenum in Icelandic geothermal waters. Contributions to Mineralogy and Petrology, 90, 179-189.
5. ARNÓRSSON, S. & ÓSKARSSON, N. 2007. Molybdenum and tungsten in volcanic rocks and in surface and< 100 C ground waters in Iceland. Geochimica et Cosmochimica Acta, 71, 284-304.
6. ASAEL, D., TISSOT, F. L. H., REINHARD, C. T., ROUXEL, O., DAUPHAS, N., LYONS, T. W., PONZEVERA, E., LIORZOU, C. & CHÉRON, S. 2013. Coupled molybdenum, iron and uranium stable isotopes as oceanic paleoredox proxies during the Paleoproterozoic Shunga Event. Chemical Geology, 362, 193-210.
7. BARLING, J., ARNOLD, G. L. & ANBAR, A. D. 2001. Natural mass-dependent variations in the isotopic composition of molybdenum. Earth and Planetary Science Letters, 193, 447-457.
8. BARLING, J. & ANBAR, A. D. 2004. Molybdenum isotope fractionation during adsorption by manganese oxides. Earth and Planetary Science Letters, 217, 315-329.
9. BREILLAT, N., GUERROT, C., MARCOUX, E. & NÉGREL, P. 2016. A new global database of δ98Mo in molybdenites: A literature review and new data. Journal of Geochemical Exploration, 161, 1-15.

10. DARLING, W. G. & ÁRMANNSSON, H. 1989. Water-rock interaction Stable isotopic aspects of fluid flow in the Krafla, Námafjall and Theistareykir geothermal systems of northeast Iceland. Chemical Geology, 76, 197-213.
11. DE RONDE, C. E. J., CHANNER, D. M. D., FAURE, K., BRAY, C. J. & SPOONER, E. T. C. 1997. Fluid chemistry of Archean seafloor hydrothermal vents: Implications for the composition of circa 3.2 Ga seawater. Geochimica et Cosmochimica Acta, 61, 4025-4042.
12. GISLASON, S.R. & EUGSTER, H.P. 1987. Meteoric water-basalt interactions: II. A field study in NE Iceland. Geochim. Cosmochim. Acta 51, pp. 2841-2855.
13. GOLDBERG, T., ARCHER, C., VANCE, D. & POULTON, S. W. 2009. Mo isotope fractionation during adsorption to Fe (oxyhydr)oxides. Geochimica et Cosmochimica Acta, 73, 6502-6516.
14. GOLDBERG, T., GORDON, G., IZON, G., ARCHER, C., PEARCE, C. R., MCMANUS, J., ANBAR, A. D. & REHKÄMPER, M. 2013. Resolution of inter-laboratory discrepancies in Mo isotope data: an intercalibration. Journal of Analytical Atomic Spectrometry, 28, 724-735.
15. GREBER, N. D., PETTKE, T. & NÄGLER, T. F. 2014. Magmatic–hydrothermal molybdenum isotope fractionation and its relevance to the igneous crustal signature. Lithos, 190–191, 104-110.
16. GUDMUNDSSON, B. T. & ARNÓRSSON, S. 2002. Geochemical monitoring of the Krafla and Námafjall geothermal areas, N-Iceland. Geothermics, 31, 195-243.
17. GUDMUNDSSON, B. T. & ARNÓRSSON, S. 2005. Secondary mineral–fluid equilibria in the Krafla and Námafjall geothermal systems, Iceland. Applied Geochemistry, 20, 1607-1625.

18. HURTIG, N. C. & WILLIAMS-JONES, A. E. 2014. An experimental study of the solubility of MoO 3 in aqueous vapour and low to intermediate density supercritical fluids. Geochimica et Cosmochimica Acta, 136, 169-193.
19. KAASALAINEN, H. & STEFÁNSSON, A. 2012. The chemistry of trace elements in surface geothermal waters and steam, Iceland. Chemical Geology, 330–331, 60-85.
20. KAASALAINEN, H., STEFANSSON, A. & DRUSCHEL, G. K. 2016. Determination of Fe (II), Fe (III) and Fetotal in thermal water by ion chromatography spectrophotometry (IC-Vis). International Journal of Environmental Analytical Chemistry, 96, 1074-1090.
21. KENDALL, B., DAHL, T., ANABAR, A. 2016. Good Golly, Why Moly? The Stable Isotope Geochemistry of Molybdenum, Reviews in Mineralogy and Geochemistry, 82, 683-732.
22. KING, E. K., THOMPSON, A., CHADWICK, O. A. & PETT-RIDGE, J. C. 2016. Molybdenum sources and isotopic composition during early stages of pedogenesis along a basaltic climate transect. Chemical Geology, 445, 54-67.
23. KRISTINSSON, S. G., ÓSKARSSON, F., ÓLAFSSON, M. & ÓLADÓTTIR, A. A. 2014. Háhitasvæðin í Kröflu, Námafjalli og á Þeistareykjum: Vöktun á yfirborðsvirkni og grunnvatni árið 2014 (The high temperature areas of Krafla, Námafjall and Þeistareyki: monitoring of groundwater an surface activity in 2014). ÍSOR (Íslenskar Orkurannsóknir) Icelandic GeoSurvey. LV-2014-132 ÍSOR2014/058
24. LEYBOURNE, M. I. & CAMERON, E. M. 2008. Source, transport, and fate of rhenium, selenium, molybdenum, arsenic, and copper in groundwater associated with porphyry–Cu deposits, Atacama Desert, Chile. Chemical Geology, 247, 208-228.

25. LOWELL, R. P. & KELLER, S. M. 2003. High-temperature seafloor hydrothermal circulation over geologic time and Archean banded iron formations. Geophysical research letters, 30.
26. MCMANUS, J., NÄGLER, T. F., SIEBERT, C., WHEAT, C. G. & HAMMOND, D. E. 2002. Oceanic molybdenum isotope fractionation: Diagenesis and hydrothermal ridge-flank alteration. Geochemistry, Geophysics, Geosystems, 3, 1-9.
27. MILLER, C. A., PEUCKER-EHRENBRINK, B., WALKER, B. D. & MARCANTONIO, F. 2011. Re-assessing the surface cycling of molybdenum and rhenium. Geochimica et Cosmochimica Acta, 75, 7146-7179.
28. MOORE, W. S. 1996. Large groundwater inputs to coastal waters revealed by 226Ra enrichments. Nature, 380, 612-614.
29. Nägler, TF, Anbar, AD, Archer, C, Goldberg, T, Gordon, GW, Greber, ND, Siebert, C, Sohrin, Y & Vance, D 2014, 'Proposal for an International Molybdenum Isotope Measurement Standard and Data Representation' Geostandards and Geoanalytical Research, vol 38, no. 2, pp. 149-151.
30. NAKAGAWA, Y., TAKANO, S., FIRDAUS, M. L., NORISUYE, K., HIRATA, T., VANCE, D. & SOHRIN, Y. 2012. The molybdenum isotopic composition of the modern ocean. Geochemical Journal, 46, 131-141.
31. Neely R, Þorbjörnsson D, Pearce C, Gislason S & Burton K (2015) Molybdenum Isotope Behaviour Accompanying Vapour-Phase Transport in Geothermal Systems. Goldschmidt Abstracts, 2015 2251
32. NEUBERT, N., HERI, A., VOEGELIN, A., NÄGLER, T., SCHLUNEGGER, F. & VILLA, I. 2011. The molybdenum isotopic composition in river water: constraints from small catchments. Earth and planetary science letters, 304, 180-190.

33. ÓLAFSSON, M., FRIDRIKSSON, T., HAFSTAD, T. H., GYLFADÓTTIR, S. S., ÓSKARSSON, F. & ÁRMANNSSON, H. 2015. The Groundwater in the Mývatn Area: Influence of Geothermal Utilization at Námafjall and Origin of the Warm Groundwater Component. In *Proceedings of World Geothermal Congress 2015* Melbourne, Australia 19-25.
34. ÓSKARSSON, F., ÁRMANNSSON, H., ÓLAFSSON, M., SVEINBJÖRNSDÓTTIR, Á. E. & MARKÚSSON, S. H. 2013. The Theistareykir Geothermal Field, NE Iceland: Fluid Chemistry and Production Properties. Procedia Earth and Planetary Science, 7, 644-647.
35. PARKHURST, D.L., & APPELO, C.A.J., 2013, Description of input and examples for PHREEQC version 3—A computer program for speciation, batch-reaction, one-dimensional transport, and inverse geochemical calculations: U.S. Geological Survey Techniques and Methods, book 6, chap. A43, 497 p., available only at https://pubs.usgs.gov/tm/06/a43/.
36. PATTEN, C., BARNES, S.-J., MATHEZ, E. A. & JENNER, F. E. 2013. Partition coefficients of chalcophile elements between sulfide and silicate melts and the early crystallization history of sulfide liquid: LA-ICP-MS analysis of MORB sulfide droplets. Chemical Geology, 358, 170-188.
37. PEARCE, C. R., COHEN, A. S., COE, A. L. & BURTON, K. W. 2008. Molybdenum isotope evidence for global ocean anoxia coupled with perturbations to the carbon cycle during the Early Jurassic. Geology, 36, 231-234.
38. PEARCE, C. R., COHEN, A. S. & PARKINSON, I. J. 2009. Quantitative Separation of Molybdenum and Rhenium from Geological Materials for Isotopic Determination by MC-ICP-MS. Geostandards and Geoanalytical Research, 33, 219-229.

39. PEARCE, C. R., BURTON, K. W., VON STRANDMANN, P. A., JAMES, R. H. & GÍSLASON, S. R. 2010. Molybdenum isotope behaviour accompanying weathering and riverine transport in a basaltic terrain. Earth and Planetary Science Letters, 295, 104-114.
40. PELTONEN, P., KONTINEN, A., HUHMA, H., KURONEN, U. 2008. Outokumpu revisited: New mineral deposit model for the mantle peridotite-associated Cu–Co–Zn–Ni–Ag–Au sulphide deposits. Ore Geology Reviews, 33, 559-617
41. SIEBERT, C., PETT-RIDGE, J. C., OPFERGELT, S., GUICHARNAUD, R. A., HALLIDAY, A. N. & BURTON, K. W. 2015. Molybdenum isotope fractionation in soils: Influence of redox conditions, organic matter, and atmospheric inputs. Geochimica et Cosmochimica Acta, 162, 1-24.
42. SVEINBJORNSDOTTIR, Á., ÁRMANNSSON, H., ÓLAFSSON, M., ÓSKARSSON, F., MARKÚSSON, S. & MAGNUSDOTTIR, S. 2013. The Theistareykir geothermal field, NE Iceland. Isotopic characteristics and origin of circulating fluids. Procedia Earth and Planetary Science, 7, 822-825.
43. TAYLOR S. R. and MCLENNAN, S. M. (1985) The Continental Crust: Its Composition and Evolution. Blackwell Scientific Public.
44. TOSSELL, J. A. 2005. Calculating the partitioning of the isotopes of Mo between oxidic and sulfidic species in aqueous solution. Geochimica et Cosmochimica Acta, 69, 2981-2993.
45. VOEGELIN, A. R., NÄGLER, T. F., PETTKE, T., NEUBERT, N., STEINMANN, M., POURRET, O. & VILLA, I. M. 2012. The impact of igneous bedrock weathering on the Mo isotopic composition of stream waters: Natural samples and laboratory experiments. Geochimica et Cosmochimica Acta, 86, 150-165.

46. VOEGELIN, A. R., PETTKE, T., GREBER, N. D., VON NIEDERHÄUSERN, B. & NÄGLER, T. F. 2014. Magma differentiation fractionates Mo isotope ratios: Evidence from the Kos Plateau Tuff (Aegean Arc). Lithos, 190–191, 440-448.
47. WASYLENKI, L. E., WEEKS, C. L., BARGAR, J. R., SPIRO, T. G., HEIN, J. R. & ANBAR, A. D. 2011. The molecular mechanism of Mo isotope fractionation during adsorption to birnessite. Geochimica et Cosmochimica Acta, 75, 5019-5031.
48. WILLBOLD, M. & ELLIOTT, T. 2017. Molybdenum isotope variations in magmatic rocks. Chemical Geology, 449, 253-268.
49. Wille, M., Nägler, T. F., Lehmann, B., Schröder, S., Kramers, J.D. (2008): Hydrogen sulphide release to surface waters at the Precambrian/Cambrian boundary. Nature, 453(7196), 767-769.
50. YANG, J., SIEBERT, C., BARLING, J., SAVAGE, P., LIANG, Y.-H. & HALLIDAY, A. N. 2015. Absence of molybdenum isotope fractionation during magmatic differentiation at Hekla volcano, Iceland. Geochimica et Cosmochimica Acta, 162, 126-136.

Acknowledgments

The geochemistry team at ÍSOR are thanked for sample collection along with Landsvirkjun for permission to publish the sample information. Geoff Nowell, in particular, is thanked for his generous help in the preparation and isotopic analysis of the samples and Chris Ottley for assistance with ICP-MS analysis. We acknowledge financial support from Initial Training Network, MetTrans, grant number 290336 from the European Research Council. Finally we would like to thank the three anonymous reviewers and Editor, Derek Vance, for their advice and thoughtful consideration of this manuscript.

Figure Captions:

Figure 1: Map showing the location and sampling temperatures of the Mývatn (M) and Þeistareykir (Þ) groundwater samples in the northern volcanic zone (NVZ) of Iceland. Inset A shows the two groundwater systems in relation to the major geographical features of Iceland; the main volcanic and fracture zones are shown in red and major icecaps and glaciers in white; and the black star is the Reykjanes hydrothermal system, location of the basalt samples. Inset B depicts the Þesitaryekir sampling locations (diamonds) and inset C the Mývatn groundwater samples (circles). The Mývatn samples overly a simple base map including the Krafla caldera features (Gudmundsson & Arnorsson 2002) and the groundwater types (I-VI) defined on the basis of their chemistry by Ármannsson et al. (2000). The cold growdwaters for both systems are sourced from as far south as Vatnajöjull (VJ) glacier.

Figure 2: pH-Eh diagram at 25°C and 105 Pa for the S-O-H system with available, oxidised, Mo data superimposed. Mo speciation below the SO_4^{2-} - H_2S transition is not well characterised although it is thought to be dominated by oxythiomolybdate species ($MoO_{4-x}S_x^{2-}$). Calculated in situ pH and Eh for the groundwater samples are plotted: filled circles are Mývatn groundwaters whilst the diamonds are from Þeistareykir; blue denotes a sampling temperature of less than 10°C and red, hydrothermally influenced waters. Despite a range in Eh values, all samples are dominated by MoO_4^{2-}. Calculations are based on the minteq.v4 database within PHREEQC (Parkhurst & Appelo 2013). The stability field for water lies between the two dashed lines.

Figure 3: Molybdenum versus SO_4^{2-} in precipitation, surface waters, groundwaters, and geothermal systems after Miller et al. (2011). The grey data are from the literature: river and precipitation data from Miller et al. (2011) and Neubert et al. (2011), geothermal from Kaasalainen & Stefánsson (2012) and Arnórsson & Ívarsson (1985), and groundwaters from Leybourne & Cameron (2008). The coloured data are from this study: filled circles are Mývatn groundwaters whilst the diamonds are from Þeistareykir, blue denotes a sampling temperature of less than 10°C and red, hydrothermally influenced waters. After Miller et al. (2011), a best-fit regression line, forced through the origin, is plotted through the groundwaters from this study (excluding the group V waters as described in the text) and the resulting slope and coefficient of determination (R^2) are shown and are in agreement with those reported in Miller et al. (2011) for rivers ($y = 0.01x$, $R^2 = 0.69$).

Figure 4: Mo concentration and isotope data for terrestrial groundwaters including those that are geothermally affected (red). All data are from this study save for the four Hawaiian groundwaters (blue crosses) from King et al. (2016). For reference, values for a range of Icelandic basalts (Table 2 & Yang et al., 2015) and the mean global river composition (Archer & Vance 2008) are plotted.

Figure 5: Relationship between Mo isotopes and Mo and SO_4^{2-} concentrations in the Mývatn groundwater system. Cold groundwaters (sampling temperature <10°C) are depicted in blue whilst those that are geothermally influenced are shown in red. The distinct group V waters (as discussed in the main text) are open red circles. For reference, the Mo isotopic range of Icelandic basalts ($\delta^{98}Mo_{BASALT}$ = -0.1 to -0.4‰) is shown as the shaded band (Table 2). There are two mixing lines, both have a common cold groundwater endmember (M07) but two distinct geothermal endmembers: one low [Mo], mid-range SO_4^{2-}, and isotopically heavy (M14, dashed line) and one high [Mo], high SO_4^{2-}, and heavy Mo isotopes (M17solid line).

Figure 6: Log pCO_2 for all of the groundwaters. The pH and pCO_2 are calculated for the sampling conditions using PHREEQC (Parkhurst & Appelo 2013) and the minteq.v4 database. The reference line is the pCO_2 of the modern atmosphere.

Figure 7: Basalt primary mineral saturation indices (SI) in the Mývatn and Þeistareykir groundwaters plotted against both the Mo isotope composition and sampling temperature of the waters. Saturation indices are calculated using the PHREEQC database and SI >0 suggests that the mineral phase is stable whilst SI <0 indicates the possibility of dissolution. The grey arrows highlight the potential increase in olivine dissolution over plagioclase dissolution with increasing temperature.

Figure 8: Molybdenum isotope compositions for sources of Mo to the modern oceans. The grey bars denote the range whilst the black diamonds show mean values and the stars are minimum estimates of the hydrothermal endmembers. The grey outline for the high temperature fluids shows the range of values measured for the mixed fluids in this study. River data is summarised in Kendall et al. (2016), Hawaii groundwater data from King et al. (2016), and the low temperature hydrothermal fluids from McManus et al. (2002). In addition, the individual sulfide values from this study are plotted (black squares) with the entire molybdenite range (from Breillat et al., 2016) for comparison. * denotes data from this study.

Fig. 1

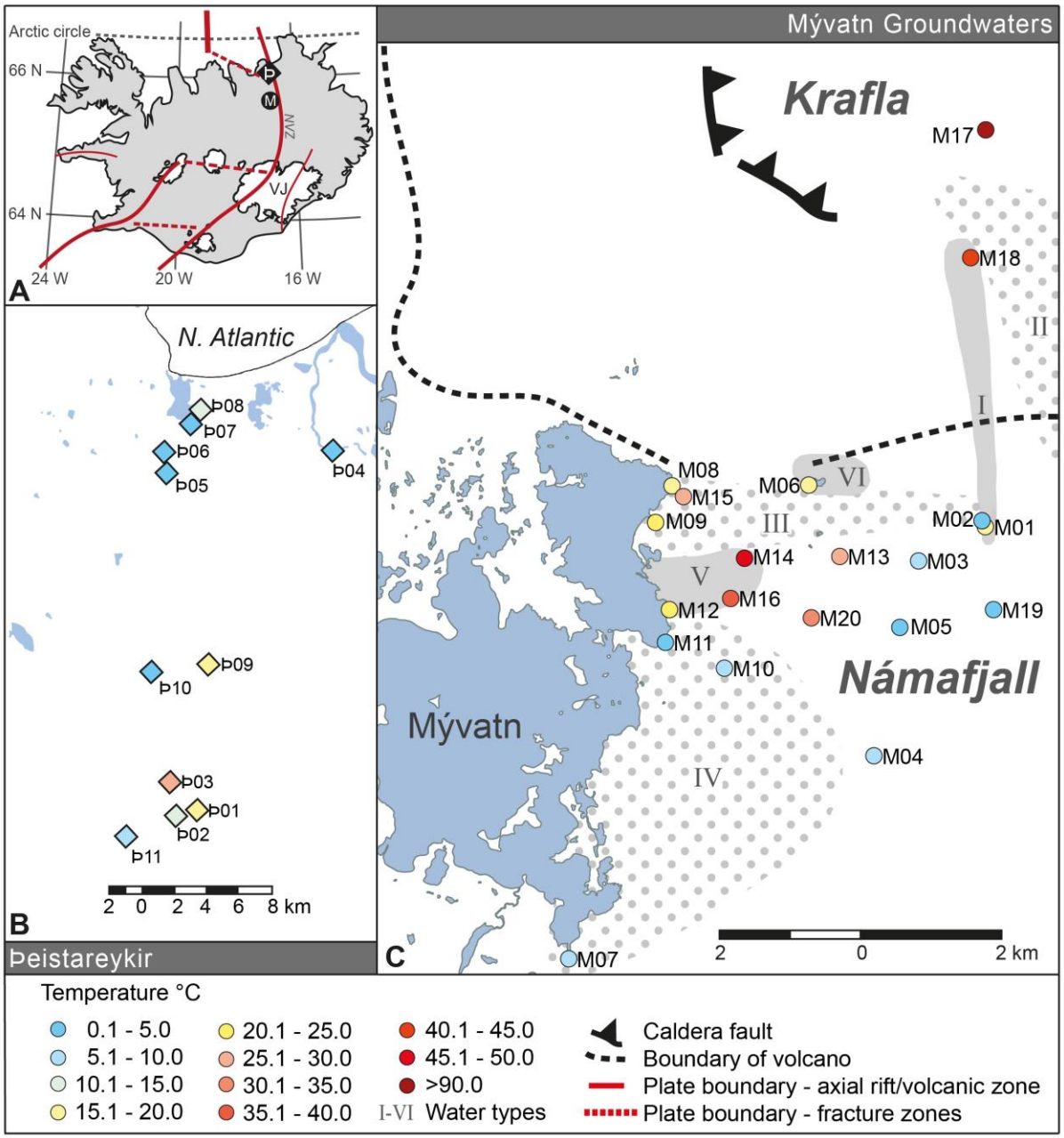
Mývatn Groundwaters
Krafla
Námafjall
Mývatn
N. Atlantic
Arctic circle
66 N
64 N
24 W
20 W
16 W
NVZ
VJ
A
B
C
Þ08
Þ07
Þ06
Þ05
Þ04
Þ09
Þ10
Þ03
Þ01
Þ02
Þ11
2 0 2 4 6 8 km
M17
M18
M08
M15
M06
M09
M02
M01
M14
M13
M03
M12
M16
M20
M05
M19
M11
M10
M04
M07
I
II
III
IV
V
VI
2 0 2 km
Þeistareykir
Temperature °C
0.1 - 5.0
5.1 - 10.0
10.1 - 15.0
15.1 - 20.0
20.1 - 25.0
25.1 - 30.0
30.1 - 35.0
35.1 - 40.0
40.1 - 45.0
45.1 - 50.0
>90.0
I-VI Water types
Caldera fault
Boundary of volcano
Plate boundary - axial rift/volcanic zone
Plate boundary - fracture zones

Fig. 2

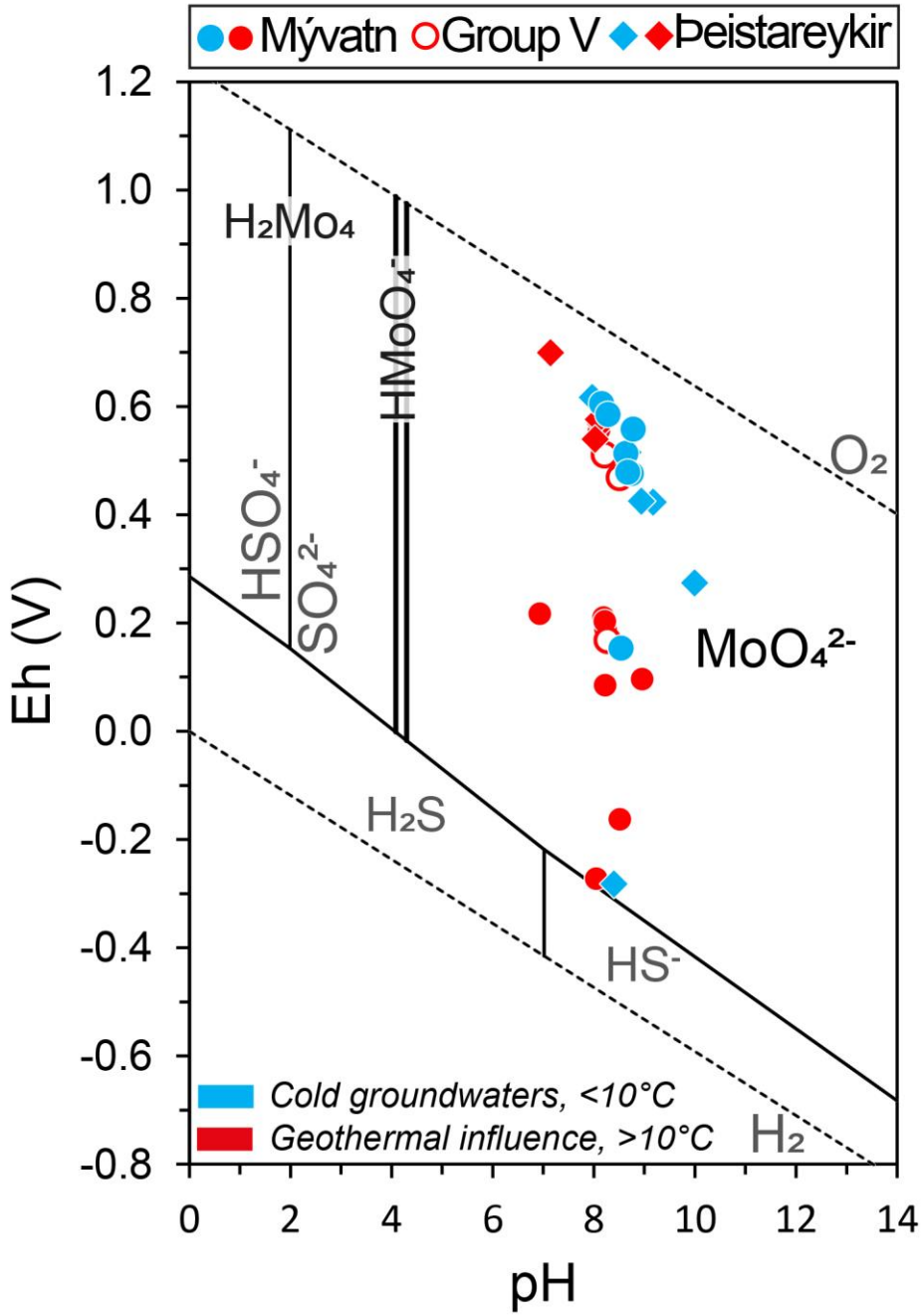
Mývatn
Group V
Þeistareykir
1.2
1.0
0.8
0.6
0.4
0.2
0.0
-0.2
-0.4
-0.6
-0.8
Eh (V)
0
2
4
6
8
10
12
14
pH
H2Mo4
HMoO4-
HSO4-
SO4 2-
O2
MoO4 2-
H2S
HS-
H2
Cold groundwaters, <10°C
Geothermal influence, >10°C

Fig. 3

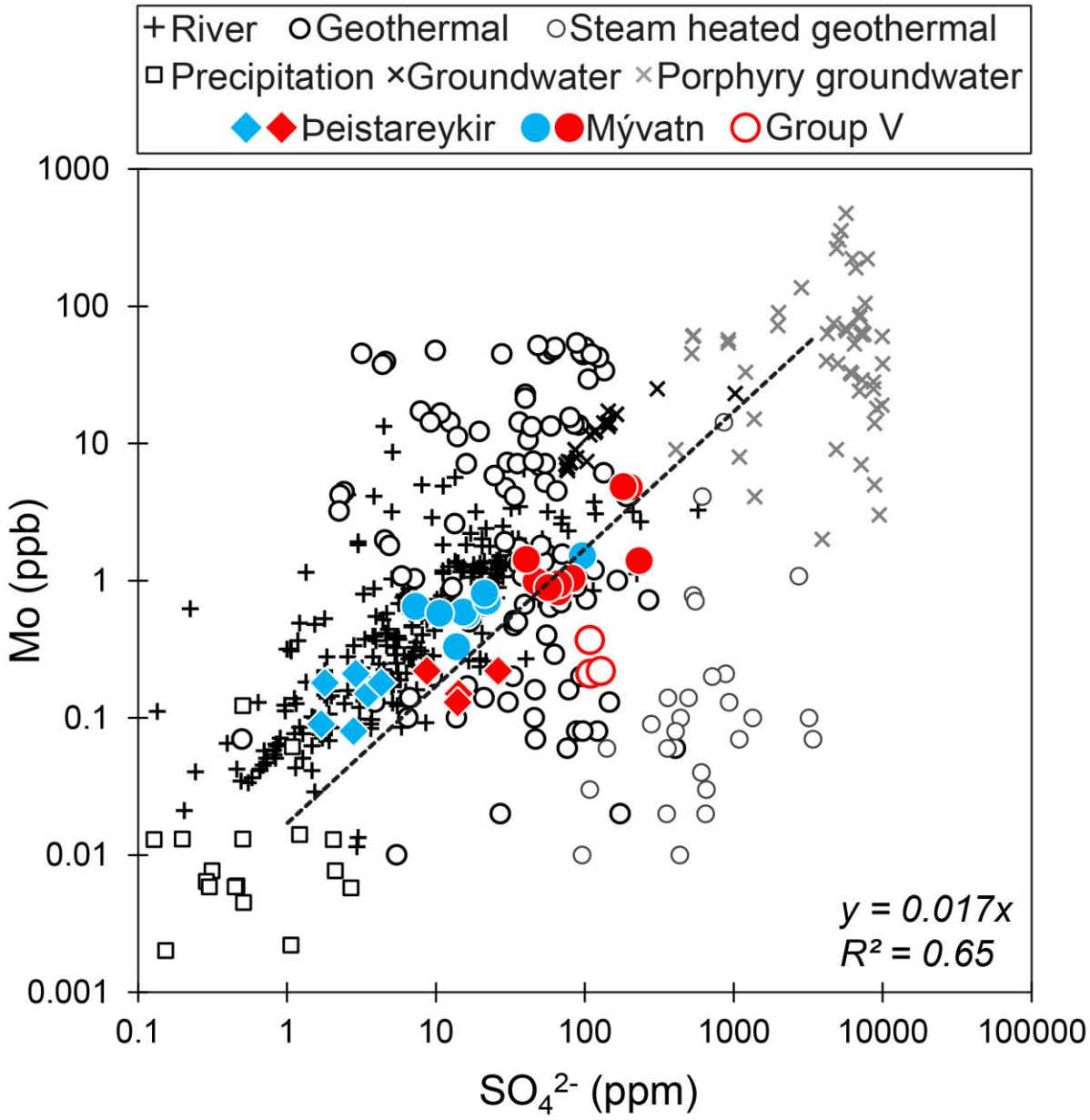
River
Geothermal
Steam heated geothermal
Precipitation
Groundwater
Porphyry groundwater
Þeistareykir
Mývatn
Group V
Mo (ppb)
1000
100
10
1
0.1
0.01
0.001
0.1
1
10
100
1000
10000
100000
SO4 2- (ppm)
y = 0.017x
R² = 0.65

Fig. 4

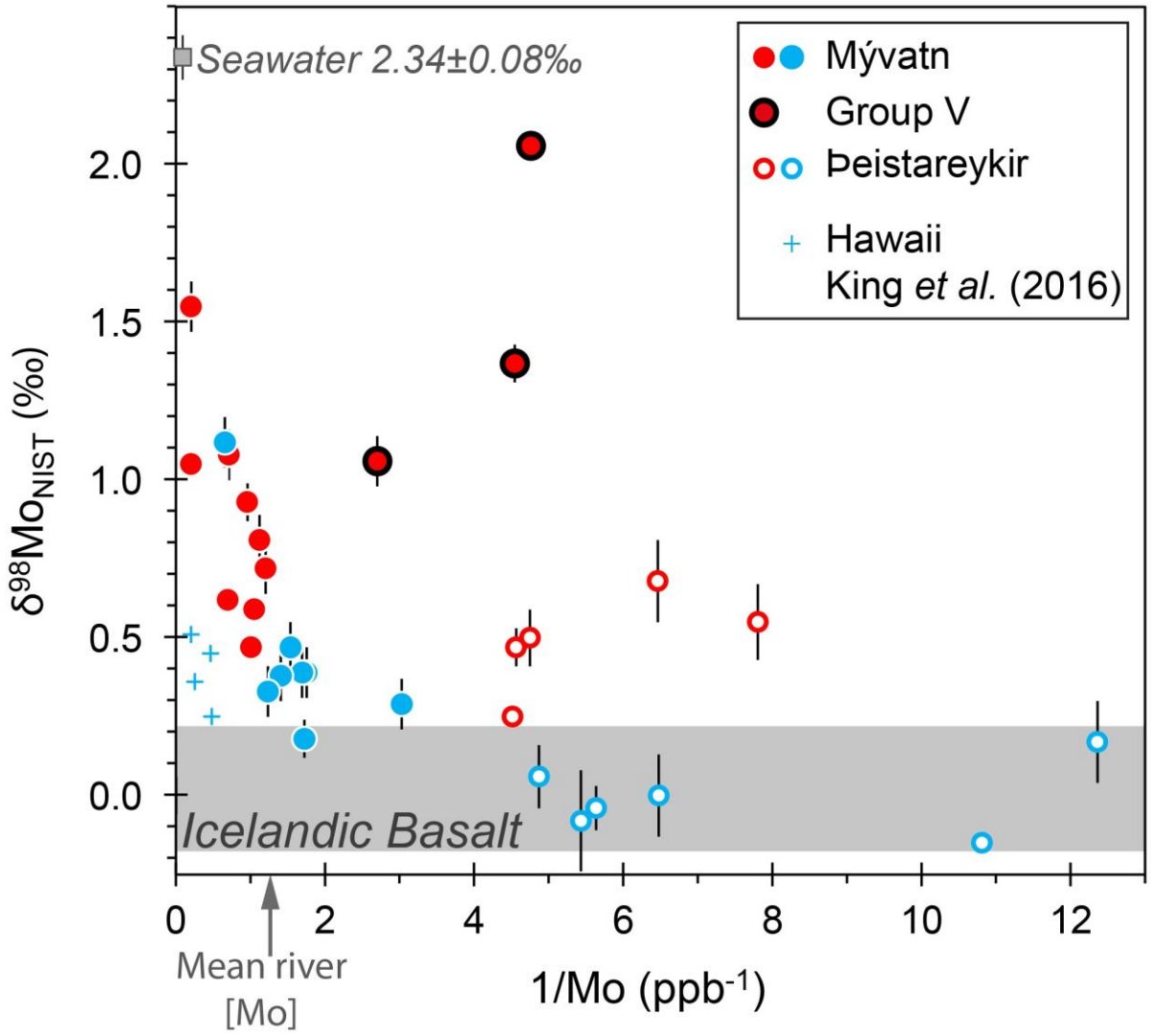
Seawater 2.34±0.08‰
Mývatn
Group V
Þeistareykir
Hawaii
King et al. (2016)
Icelandic Basalt
Mean river [Mo]
δ98MoNIST (‰)
1/Mo (ppb-1)
2.0
1.5
1.0
0.5
0.0
0
2
4
6
8
10
12

Fig. 5

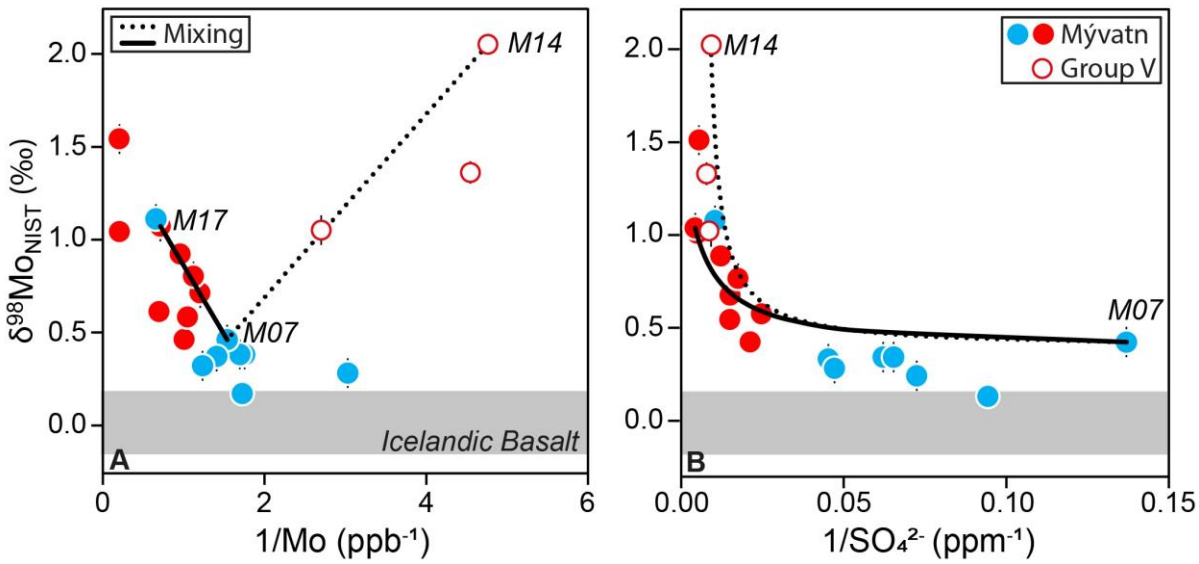
Mixing
M14
M17
M07
Icelandic Basalt
A
δ98MoNIST (‰)
1/Mo (ppb-1)
Mývatn
Group V
B
1/SO4 2- (ppm-1)

Fig. 6

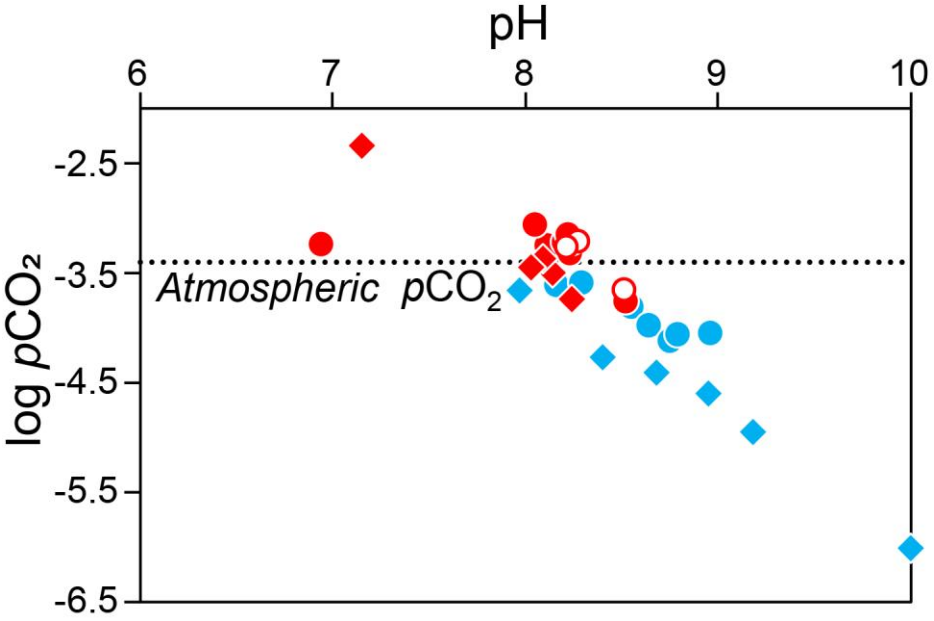
pH
Atmospheric pCO2
log pCO2

Fig. 7

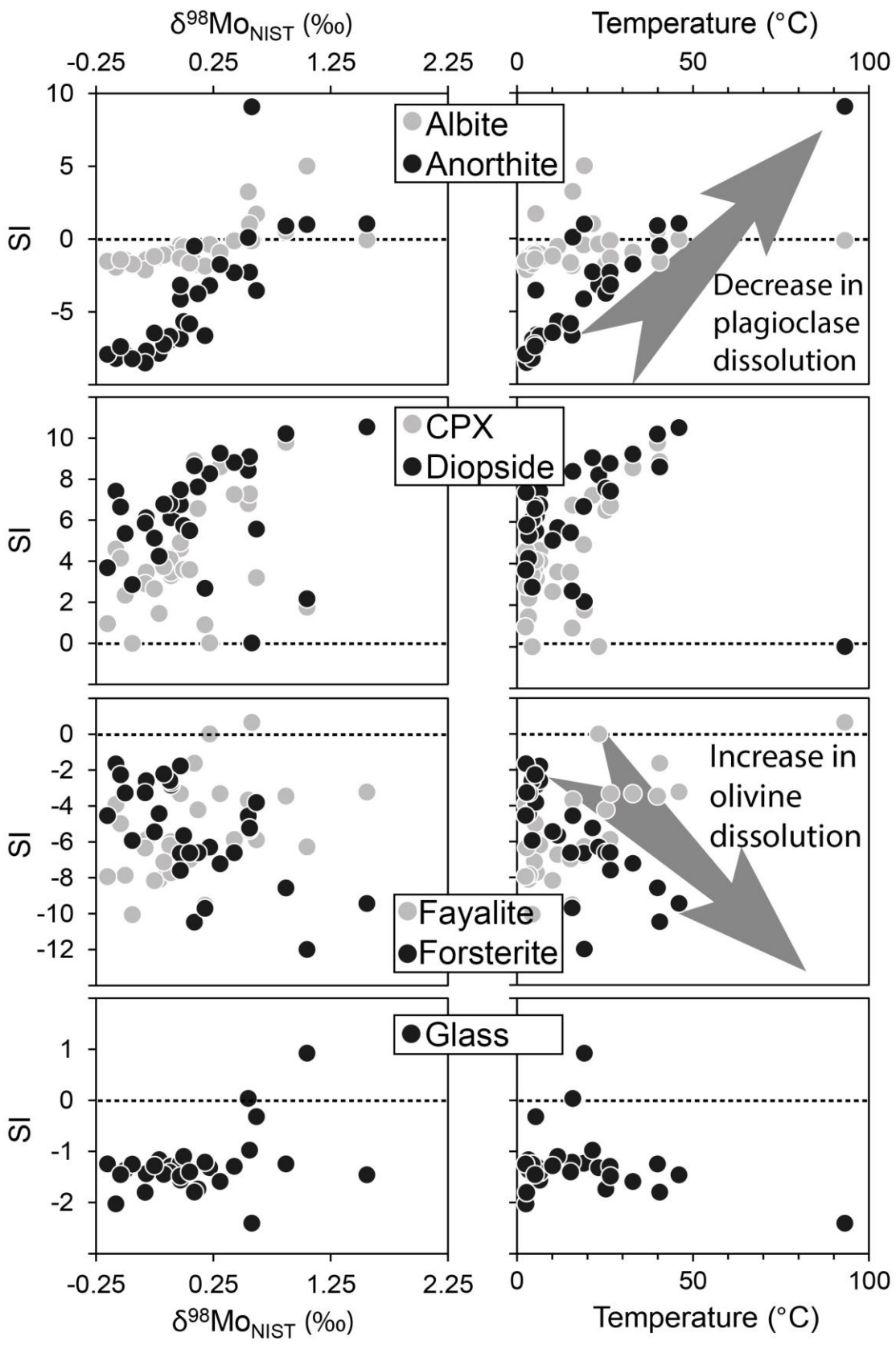
δ98MoNIST (‰)
-0.25
0.25
1.25
2.25
Temperature (°C)
0
50
100
SI
Albite
Anorthite
Decrease in plagioclase dissolution
CPX
Diopside
Increase in olivine dissolution
Fayalite
Forsterite
Glass

Fig. 8

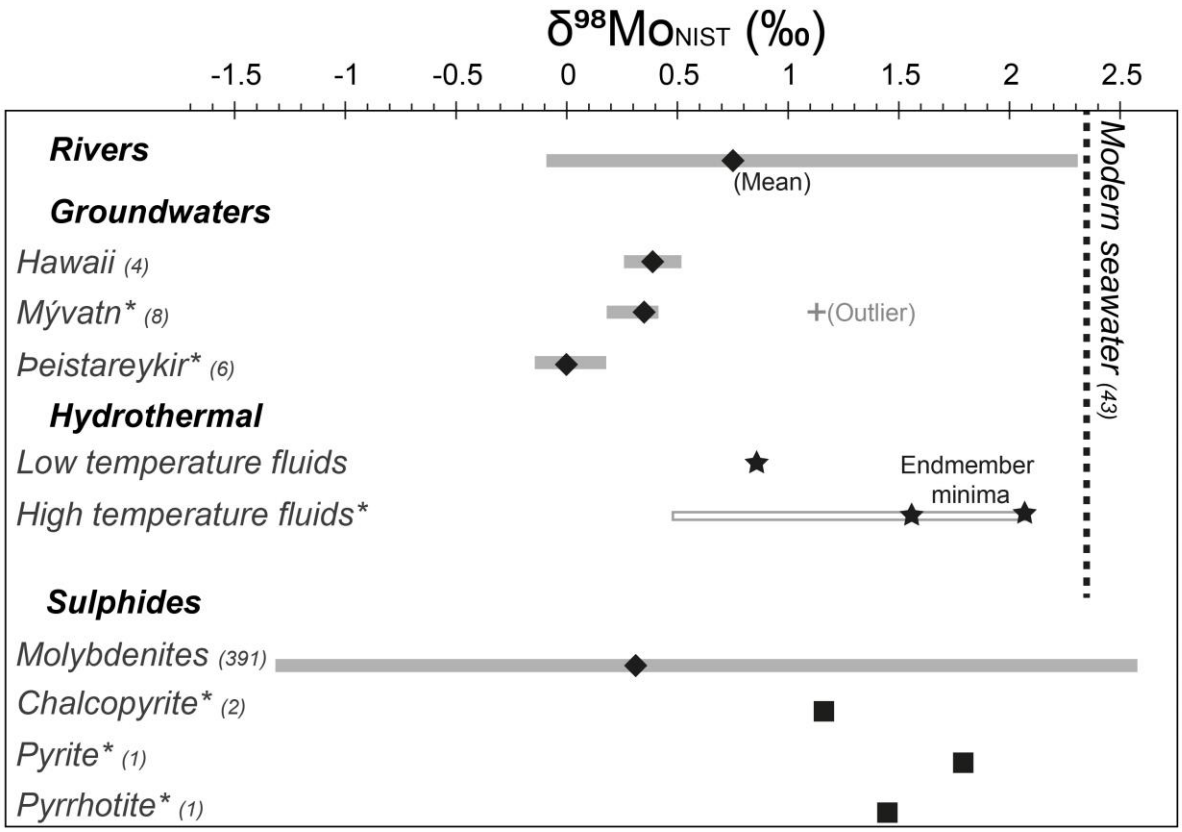
δ98MoNIST (‰)
-1.5
-1
-0.5
0
0.5
1
1.5
2
2.5
Rivers
(Mean)
Groundwaters
Hawaii (4)
Mývatn* (8)
+(Outlier)
Þeistareykir* (6)
Hydrothermal
Low temperature fluids
Endmember minima
High temperature fluids*
Sulphides
Molybdenites (391)
Chalcopyrite* (2)
Pyrite* (1)
Pyrrhotite* (1)
Modern seawater (43)

Table 1: Selected data for Mývatn and Þeistareykir groundwaters (δ^{98}Mo relative to NIST= +0.25‰).

		Temp	pH* *in situ*	Eh*	Na	Mg	Cl	H_2S	SO_4	Mo	δ^{98}Mo		2 SD	n
		°C		V	ppm	ppm	ppm	ppm	ppm	ppb	‰			
MÝVATN GROUNDWATERS														
M01	Hliðardalslækur	15.9	8.23	0.08	91.3	12.50	26.00	b.d.l	199.00	4.81	1.05	±	0.04	4(2)
M02	AB-2	3.3	8.16	0.60	11.2	5.15	4.36	b.d.l	13.80	0.331	0.29	±	0.08	2
M03	LUD-4	5.4	8.29	0.58	53.6	9.20	12.30	b.d.l	96.20	1.52	1.12	±	0.08	2
M04	LUD-2	5.6	8.55	0.15	18.6	7.60	5.74	b.d.l	16.10	0.565	0.39	±	0.08	2
M05	LUD-3	4.5	8.64	0.51	15.3	7.07	5.29	b.d.l	15.30	0.594	0.39	±	0.08	2
M06	Svelgur	19.2	6.94	0.22	119.0	1.21	54.00	0.05	181.00	4.85	1.55	±	0.08	2
M07	Garðslind	6.5	8.96	0.10	17.4	4.64	2.11	b.d.l	7.33	0.654	0.47	±	0.08	2
M08	Bjarg	19.0	8.11	0.56	44.3	4.02	9.71	b.d.l	47.10	0.988	0.47	±	0.01	3
M09	Helgavogur	23.3	8.24	0.19	52.3	5.56	8.04	b.d.l	66.20	0.832	0.72	±	0.08	3
M10	Hverfjallsgjá	6.5	8.75	0.48	21.5	6.84	5.08	b.d.l	22.10	0.713	0.38	±	0.08	2
M11	Vogaflói	5.0	8.79	0.56	21.1	6.26	4.75	b.d.l	21.20	0.812	0.33	±	0.08	2
M12	Langivogur	21.5	8.51	0.47	76.9	3.64	15.10	b.d.l	108.00	0.371	1.06	±	0.08	2
M13	LUD-10	25.3	8.20	0.21	37.3	8.57	4.54	b.d.l	40.50	1.43	0.62	±	0.03	3
M14	Grjótagjá	46.1	8.27	0.17	86.3	3.09	17.70	0.08	109.00	0.206	2.06	±	0.03	5(2)
M15	Stóragjá	26.5	8.23	0.20	61.8	5.58	9.57	b.d.l	81.90	1.04	0.93	±	0.06	3
M16	Vogagjá	40.0	8.21	0.51	88.0	2.49	17.50	b.d.l	128.00	0.219	1.37	±	0.06	3
M17	Skiljustöð	93.2	8.52	-0.16	250.0	0.01	81.30	22.4	232.00	1.4	1.08	±	0.08	2
M18	AE-10	40.6	8.05	-0.27	42.0	0.99	4.09	0.03	66.80	0.954	0.59	±	0.01	3
M19	LUD-5	4.3	8.68	0.48	13.6	6.55	4.88	b.d.l	10.60	0.579	0.18	±	0.06	3
M20	LUD-6	33.0	8.22	0.51	51.7	7.11	5.67	b.d.l	57.00	0.888	0.81	±	0.08	5(2)
ÞEISTAREYKIR GROUNDWATERS														
Þ01	Þeistareykir-vatnsból	15.7	7.15	0.70	15.2	5.68	5.81	b.d.l	14.20	0.176	0.68	±	0.13	3
Þ02	Þeistareykir-Sæluhús	11.6	8.14	0.57	20.8	3.69	7.41	b.d.l	26.10	0.235	0.50	±	0.08	2
Þ03	ÞR-5	26.6	8.09	0.58	20.8	3.68	7.45	b.d.l	26.20	0.283	0.47	±	0.06	3
Þ04	Krossdalur	3.4	8.68	0.52	9.3	2.67	8.73	b.d.l	3.50	0.181	0.00	±	0.08	2
Þ05	Fjöll - lind	2.6	10.00	0.27	16.3	0.05	7.84	b.d.l	4.26	0.209	-0.08	±	0.08	2
Þ06	Fjöll - vatnsból	2.8	9.18	0.42	11.9	0.42	10.40	b.d.l	2.76	0.103	0.17	±	0.08	2
Þ07	Lón	4.4	7.97	0.62	8.7	2.59	7.68	b.d.l	2.91	0.255	0.06	±	0.10	3
Þ08	Rifós - Tangabrunnur	10.2	8.24	0.59	14.8	3.41	10.00	b.d.l	8.73	0.269	0.25	±	0.03	3
Þ09	ÞR-15	15.3	8.03	0.54	13.0	3.91	7.50	b.d.l	14.00	0.171	0.55	±	0.12	3
Þ10	ÞR-8	2.5	8.40	-0.28	6.9	1.95	6.95	0.03	1.71	0.097	-0.15	±	0.08	2
Þ11	ÞR-16	5.2	8.95	0.42	8.6	3.37	5.45	b.d.l	1.84	0.189	-0.04	±	0.07	3
IAPSO seawater										10.8	2.34	±	0.08	43(17)

*Calculated using PHREEQC and the minteq.v4 database (Pankhurst and Apello, 2013) at *in situ* temperature conditions

b.d.l. - below detection limit (0.01 ppm fpr H_2S)

Errors are reported as 2 SD of the mean when n≥3 and as the 2 SD of repeat IAPSO analyses when n<3

Table 2: Selected data for basalt and sulphide samples

		Mo ppm	δ^{98}Mo ‰		2 SD	n
ICELANDIC BASALT*						
RN09-642		1.007	-0.06	±	0.06	4 (2)
RN09-900		0.242	-0.12	±	0.08	2
RN09-1102		0.135	0.00	±	0.08	2
RN09-1200	(Hyaloclastite)	4.665	0.16	±	0.03	3 (2)
SULPHIDES, Outokumu Finland						
279-1	Chalcopyrite	38.11	1.17	±	0.03	4
279-8	Chalcopyrite	37.97	1.15	±	0.03	3
279-9	Pyrite	0.074	1.80	±	0.08	1
279-10	Pyrrhotite	0.048	1.46	±	0.08	1

δ^{98}Mo relative to NIST= +0.25‰

Errors are reported as 2 SD of the mean when n≥3 and as the 2 SD of repeat IAPSO analyses when n<3

*Bulk rock measurements